AIP | Applied Physics Letters

ZnO / Mg 0.2 Zn 0.8 O coaxial nanorod heterostructures for high-performance electronic nanodevice applications

Chul-Ho Lee, Jinkyoung Yoo, Yong-Joo Doh, and Gyu-Chul Yi

Citation: Applied Physics Letters **94**, 043504 (2009); doi: 10.1063/1.3075606
View online: http://dx.doi.org/10.1063/1.3075606
View Table of Contents: http://scitation.aip.org/content/aip/journal/apl/94/4?ver=pdfcov
Published by the AIP Publishing

Articles you may be interested in
Excitonic origin of enhanced luminescence quantum efficiency in MgZnO/ZnO coaxial nanowire heterostructures
Appl. Phys. Lett. **100**, 223103 (2012); 10.1063/1.4721519

Synthesis of high quality n -type CdS nanobelts and their applications in nanodevices
Appl. Phys. Lett. **89**, 203120 (2006); 10.1063/1.2387982

High-performance ZnO nanowire field effect transistors
Appl. Phys. Lett. **89**, 133113 (2006); 10.1063/1.2357013

Local structure around Ga in ultrafine GaN ∕ ZnO coaxial nanorod heterostructures
Appl. Phys. Lett. **88**, 111910 (2006); 10.1063/1.2185627

Heteroepitaxal fabrication and structural characterizations of ultrafine GaN/ZnO coaxial nanorod heterostructures
Appl. Phys. Lett. **84**, 3612 (2004); 10.1063/1.1738180

Want to publish your paper in the
#1 MOST CITED journal in applied physics?
With Applied Physics Letters, you can.
AIP | Applied Physics Letters
THERE'S POWER IN NUMBERS. Reach the world with AIP Publishing.

This article is copyrighted as indicated in the article. Reuse of AIP content is subject to the terms at: http://scitation.aip.org/termsconditions. Downloaded to IP: 141.223.173.110 On: Wed, 22 Apr 2015 05:35:35

$ZnO/Mg_{0.2}Zn_{0.8}O$ coaxial nanorod heterostructures for high-performance electronic nanodevice applications

Chul-Ho Lee,[1] Jinkyoung Yoo,[1] Yong-Joo Doh,[1] and Gyu-Chul Yi[2,a)]
[1]*Department of Materials Science and Engineering and National Creative Research Initiative Center for Semiconductor Nanorods, POSTECH, Pohang, Gyeongbuk 790-784, Republic of Korea*
[2]*Department of Physics and Astronomy and National Creative Research Initiative Center for Semiconductor Nanorods, Seoul National University, Seoul 151-747, Republic of Korea*

(Received 1 December 2008; accepted 7 January 2009; published online 29 January 2009)

We report on fabrication and electrical characteristics of field effect transistors (FETs) based on $ZnO/Mg_{0.2}Zn_{0.8}O$ coaxial nanorod heterostructures. As compared to bare ZnO nanorod FETs, coaxial nanorod heterostructure FETs exhibited the enhanced mobility ($\sim 110\ cm^2/V\ s$), superior subthreshold swing ($\sim 200\ mV/decade$), and negligibly small hysteresis to demonstrate very stable operation of high-performance nanorod FETs. *In situ* surface passivation and carrier confinement effects provided by heteroepitaxially grown $Mg_{0.2}Zn_{0.8}O$ shell layer are presumably responsible for the highly enhanced device performance. © *2009 American Institute of Physics*.
[DOI: 10.1063/1.3075606]

Tremendous demand has arisen for fabrication of field effect transistors (FETs) with high carrier mobility, large current on/off ratio, and small subthreshold swing for transparent electronic device applications.[1] Despite recent progress in the conventional top-down approach based on heteroepitaxial thin film growth, lithography, and etching processes, the top-down approach allows the use of only lattice-matched single-crystal substrates for high-quality thin film growth. This problem may be resolved by a bottom-up approach using nanomaterials for device fabrication.[2,3] The bottom-up method to use metal oxide nanostructures has recently demonstrated the ability to exploit nanostructures as building blocks for transparent device applications.[4,5] In particular, high-quality ZnO nanorods have been employed for fabricating FETs[6] and logic gates.[7] The device characteristics of ZnO nanorod FETs are significantly enhanced by passivating the ZnO surfaces with an insulating polymer[6,8] and inorganic dielectric layers[9] because the high-density surface states of metal oxide nanostructures cause hysteresis in the electrical characteristics[10,11] and reduce minority carrier lifetime.[12] However, significantly better device performance is expected with the use of heteroepitaxial $ZnO/Mg_{1-x}Zn_xO$ coaxial nanorod heterostructures. Here, we report the electrical characteristics of heteroepitaxial $ZnO/Mg_{0.2}Zn_{0.8}O$ coaxial nanorod heterostructures and their FET applications.

Single-crystal ZnO nanorods and heteroepitaxial $ZnO/Mg_{0.2}Zn_{0.8}O$ coaxial nanorod heterostructures were employed to fabricate high-performance nanorod FETs. In these experiments, the diameters of core ZnO nanorods ranged from 20 to 40 nm, while the $Mg_{0.2}Zn_{0.8}O$ shell layer thickness ranged from 3 to 6 nm. Details of the growth as well as the structural and optical characteristics of bare ZnO nanorods and $ZnO/Mg_{0.2}Zn_{0.8}O$ coaxial nanorod heterostructures are described elsewhere.[13] After the oxide nanostructures were prepared using catalyst-free metal-organic vapor phase epitaxy, they were dispersed on a 300-nm-thick SiO_2/heavily doped Si substrate, which was used as a back-gate electrode, as illustrated in Fig. 1(a). Figure 1(b) shows a scanning electron microscopy image of a typical nanorod FET. Micropatterns for source and drain electrodes with a channel length of 0.8–1.5 μm were made by e-beam lithography, followed by metal evaporation of the Ti/Au (60/40 nm) layers and lift-off processes. The as-fabricated devices exhibited highly resistive current–voltage ($I_{ds}-V_{ds}$) characteristics. To obtain good Ohmic contacts between the ZnO and Ti metal layers, a rapid thermal annealing process was performed in an O_2 atmosphere at 300 °C for 4 min. To conduct a fair comparison of the electrical characteristics between bare ZnO nanorod and $ZnO/Mg_{0.2}Zn_{0.8}O$ coaxial nanorod heterostructure FETs, bare ZnO nanorods with similar dimensions to those for core ZnO in the coaxial nanorod heterostructures were grown under the same growth conditions and same processes as employed for fabricating the device.

We compared the gate voltage (V_g)-dependent current (I_{ds}) characteristic curves of $ZnO/Mg_{0.2}Zn_{0.8}O$ coaxial nanorod heterostructure FETs with bare ZnO nanorod FETs at room temperature. Although both FETs exhibited typical transistor characteristics with a large current on/off ratio of $\sim 10^5$, Fig. 2 clearly shows that the device characteristics for coaxial nanorod FETs were significantly better than those of bare nanorod FETs. Most distinctive improvements were observed in the transconductance (g_m) and field effect mobility (μ_{FE}), which are key parameters. From the $I_{ds}-V_g$ characteristic curve where V_{ds}=0.5 V, the normalized $g_m(=dI_{ds}/dV_g)$ for coaxial nanorod FETs had an estimated

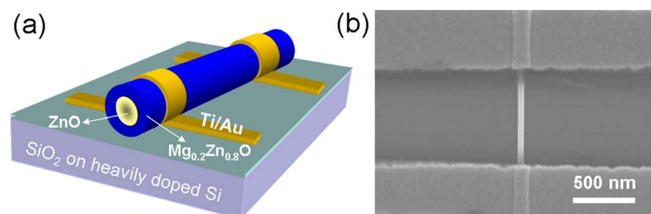

FIG. 1. (Color online) (a) Schematic diagram and (b) typical scanning electron microscopy image of $ZnO/Mg_{0.2}Zn_{0.8}O$ coaxial nanorod heterostructure FETs.

[a)]Author to whom correspondence should be addressed. Electronic mail: gyuchul.yi@gmail.com.

 © 2009 American Institute of Physics

This article is copyrighted as indicated in the article. Reuse of AIP content is subject to the terms at: http://scitation.aip.org/termsconditions. Downloaded to IP: 141.223.173.110 On: Wed, 22 Apr 2015 05:35:35

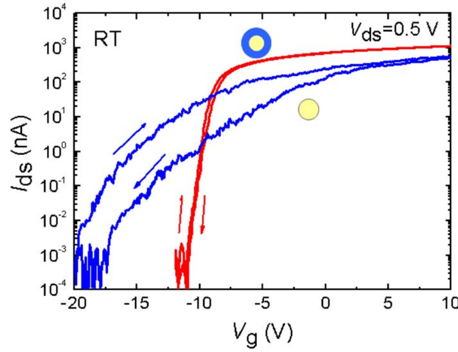

FIG. 2. (Color online) Semi-log plot of transfer characteristic ($I_{ds}-V_g$) curves of bare ZnO nanorod and coaxial nanorod heterostructure FETs at room temperature. Clockwise hysteresis loops were obtained with a typical sweep rate of 0.1 V/s for V_g.

value of 2.5 μS/μm, while the value for the bare nanorod device was 1.0 μS/μm. Using the normalized g_m values and gate capacitance coupling for the back-gate geometry,[14] the μ_{FE} value of 110 cm^2/V s was extracted for coaxial nanorod FETs, which was much higher than that of 27 cm^2/V s for bare nanorod FETs. The obtained μ_{FE} value for coaxial nanorod FETs was even higher than those for ZnO transparent thin film transistors (TFTs) (1–80 cm^2/V s)[1] and comparable to those for ZnO/$Mg_{1-x}Zn_xO$ thin film heterostructure FETs fabricated on single-crystal substrates.[15] Such improvement in μ_{FE} for coaxial nanorod FETs implies a reduction in the conduction electron scattering with the surface states and resulted from the heteroepitaxially grown $Mg_{0.2}Zn_{0.8}O$ shell layer confining carriers and reducing surface state effects.

In addition to the enhanced transconductance and carrier mobility, ZnO/$Mg_{0.2}Zn_{0.8}O$ coaxial nanorod heterostructure FETs exhibited remarkably small subthreshold swing (S) values: the average S value of 350 mV/decade and the best value of 200 mV/decade at room temperature, which are in contrast with much larger value of 1900 mV/decade for bare nanorod FETs. The S value for coaxial nanorod heterostructure FETs was much smaller than those for polymer-coated ZnO nanorod FETs,[6] ZnO TFTs,[1,15] and back-gated InAs/InP core/shell nanowire FETs.[16] As will be discussed later, the more desirable characteristics may have resulted from fewer surface and interface states in coaxial nanorod heterostructures, as compared to the number of states for bare nanorods.

Also notable in the $I_{ds}-V_g$ characteristic curves for coaxial nanorod FETs was negligible hysteresis even at room temperature as shown in Fig. 2. In contrast, the $I_{ds}-V_g$ curves for bare ZnO nanorod FETs exhibited very clear hysteresis of $\Delta V_g \sim 5$ V. The observed hysteresis, which hampers a reliable device operation, was probably associated with the surface states of the bare oxide nanorods,[6,8] molecular species adsorption onto the surfaces,[6,10] and/or interface states formed at the nanorod-SiO_2 dielectric interface.[10,11] Accordingly, the observation of negligible hysteresis in the $I_{ds}-V_g$ curves for coaxial nanorod heterostructures strongly suggests that the heteroepitaxial growth of the $Mg_{0.2}Zn_{0.8}O$ shell layer on core ZnO nanorods passivated the ZnO surface states effectively, and the possible formation of interfacial defects could be suppressed by the heteroepitaxial growth of a lattice-matched shell layer. Furthermore, conduction carriers may have been confined within the ZnO core due to the higher band gap energy of $Mg_{0.2}Zn_{0.8}O$ in comparison to ZnO. Consequently, the influence of the outer shell surface

TABLE I. Representative electrical characteristics of bare ZnO nanorod FETs and ZnO/$Mg_{0.2}Zn_{0.8}O$ coaxial nanorod heterostructure FETs measured at 78, 150, and 280 K.

	Normalized g_m (μS/μm)		Mobility (cm^2/V s)		S (mV/decade)	
	Coaxial	Bare	Coaxial	Bare	Coaxial	Bare
78 K	4.3 ± 0.5	2.3 ± 0.9	160 ± 20	50 ± 16	200 ± 31	530 ± 250
150 K	5.2 ± 1.2	2.4 ± 0.9	200 ± 45	50 ± 17	240 ± 54	540 ± 220
280 K	2.6 ± 0.5	1.3 ± 0.5	100 ± 20	30 ± 10	350 ± 29	1900 ± 100

states on electronic transport was reduced, and the stability of the nanorod FETs was enhanced.

Coaxial nanorod FET characteristics were further investigated at various temperatures from 78 K to room temperature (Table I). As good Ohmic contacts on high-quality wide band gap semiconductors were difficult to form at low temperatures, the ability to form Ohmic contacts even at 78 K was first confirmed. Figure 3(a) shows typical $I_{ds}-V_{ds}$ curves for ZnO/$Mg_{0.2}Zn_{0.8}O$ coaxial nanorod FETs, measured at 78 K and room temperature. Both curves exhibited linear and symmetric characteristics, indicating the formation of good Ohmic contacts on the coaxial nanorod heterostructures. It should be noted that the overall conductance increased from 1.6 to 2.0 μS as the temperature decreased from room temperature to 78 K, consistent with the formation of Ohmic contacts.

Additional significant temperature-dependent features of the electrical characteristics were observed from the $I_{ds}-V_g$ characteristic curves. As shown in Fig. 3(b), with decreasing temperature, the $I_{ds}-V_g$ characteristic curves of coaxial nanorod FETs exhibited a shift in threshold voltage (V_{th}) from −11 to −8.6 V and an increased normalized g_m from 2.5 to 3.9 μS/μm, corresponding to μ_{FE} values of 110 and 160 cm^2/V s. The carrier density (n) is related to V_{th} and is given by the equation of $n=C_g|V_{th}|/U$, where C_g is the gate capacitance and U is the total volume of the nanorod between two electrodes.[14] Accordingly, the reduced V_{th} at 78 K suggests that $n(\sim 1.5\times10^{18}$ cm^{-3}) at 78 K is lower than that ($\sim 1.9\times10^{18}$ cm^{-3}) at room temperature because C_g does not depend significantly on temperature. Figure 3(b) also shows that the on-state conductance in the saturation regime is higher at 78 K than that at room temperature. According to the Drude model of $\sigma=ne\mu$, where σ is the conductivity, a lower n indicates higher carrier mobility at low temperature. Other coaxial nanorod FETs also exhibited similar behavior

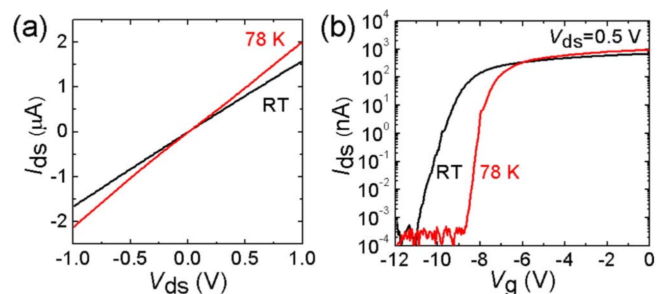

FIG. 3. (Color online) Typical (a) current–voltage ($I_{ds}-V_{ds}$) characteristic curves and (b) semi-log plot of transfer characteristic curves of a coaxial nanorod heterostructure FET at 78 K and room temperature. The transfer characteristics were measured at V_{ds}=0.5 V.

This article is copyrighted as indicated in the article. Reuse of AIP content is subject to the terms at: http://scitation.aip.org/termsconditions. Downloaded to IP: 141.223.173.110 On: Wed, 22 Apr 2015 05:35:35

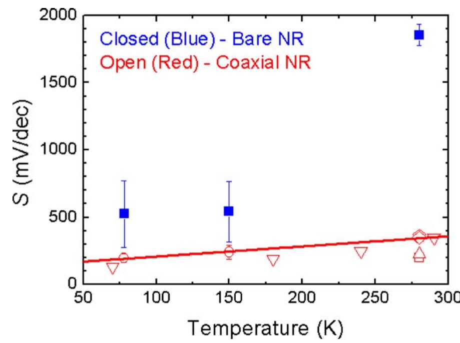

FIG. 4. (Color online) Temperature-dependent subthreshold swing (S) for coaxial nanorod heterostructure FETs. Different symbols represent different devices. The solid line shows linear fit.

in the temperature-dependent $I_{ds}-V_g$ characteristics. Such enhancement of μ_{FE} at low temperature may have resulted from the reduction in phonon scattering.[17]

In addition to the temperature dependence of the transconductance and mobility values, another distinctive feature was found in the temperature-dependent S values for coaxial nanorod FETs, as shown in Fig. 4. Coaxial nanorod FETs exhibited smaller values of S than those of bare nanorod FETs throughout the whole temperature range. In addition, their S values showed linear dependence on temperature, where S decreased from 350 mV/decade at room temperature to 200 mV/decade at 78 K. In addition, the subthreshold swing can be expressed by the following equation:[18]

$$S = \frac{dV_g}{d(\log I)} = \frac{2.3k_BT}{q}\left[1 + \frac{(C_d + C_{it})}{C_g}\right], \quad (1)$$

where k_B is the Boltzmann constant, q is the electrical charge, C_d is the depletion capacitance in the channel and C_{it} is the capacitance by surface and/or interface states. Since S is closely related to the amount of surface and/or interface states, the smaller S values for coaxial nanorod FETs compared to those for bare nanorod FETs are attributed to the fewer surface and interface states, and consequently smaller values of C_{it}. Furthermore, the linear dependence of S on temperature confirms that C_{it} should be much smaller than C_g and C_d because among those capacitances, only C_{it} is significantly dependent on temperature. In contrast to this linear behavior for coaxial nanorod FETs, bare ZnO nanorod FETs exhibited a substantial drop in S value with decreasing temperature, presumably resulting from thermal quenching of surface states. Although values of bare ZnO nanorod FETs decreased at low temperatures, they were still twice larger than those for coaxial nanorod heterostructure FETs. Accordingly, the observed temperature-dependent behavior of S strongly suggests that the improved electrical characteristics of heteroepitaxial oxide coaxial nanorod heterostructures resulted from the effective passivation of ZnO surface states and the negligibly small number of interface states between the ZnO and $Mg_{0.2}Zn_{0.8}O$ layers.

High-quality $ZnO/Mg_{0.2}Zn_{0.8}O$ coaxial nanorod heterostructures provide significant opportunities for the fabrication of high-performance oxide electronic nanodevices. Excellent electrical characteristics for coaxial nanorod heterostructure FETs, as compared with bare ZnO nanorod FETs, were observed: much higher mobility and smaller subthreshold swing values. Such desirable behavior by an oxide coaxial nanorod heterostructure device was mainly attributable to both *in situ* surface passivation and carrier confinement effects through the heteroepitaxial growth of a lattice-matched $Mg_{0.2}Zn_{0.8}O$ shell layer with a wider band gap than ZnO nanorods. These oxide coaxial nanorod heterostructures would markedly increase the versatility and power as a building block for the fabrication of numerous electrical nanodevices based on oxide heterostructures.

This work was financially supported by the National Creative Research Initiative Project (Grant No. R16-2004-004-01001-0) of the Korea Science and Engineering Foundations (KOSEF).

[1]E. Fortunato, P. Barquinha, A. Pimentel, A. Gonçalves, A. Marques, L. Pereira, and R. Martins, Thin Solid Films **487**, 205 (2005).
[2]X. Duan, MRS. Bull. **32**, 134 (2007).
[3]A. J. Baca, J.-H. Ahn, Y. Sun, M. A. Meitl, E. Menard, H.-S. Kim, W. M. Choi, D.-H. Kim, Y. Huang, and J. A. Rogers, Angew. Chem., Int. Ed. **47**, 5524 (2008).
[4]S. Ju, A. Facchetti, Y. Xuan, J. Liu, F. Ishikawa, P. Ye, C. Zhou, T. J. Marks, and D. B. Janes, Nat. Nanotechnol. **2**, 378 (2007).
[5]E. N. Dattoli, Q. Wan, W. Guo, Y. Chen, X. Pan, and W. Lu, Nano Lett. **7**, 2463 (2007).
[6]W. I. Park, J. S. Kim, G.-C. Yi, M. H. Bae, and H.-J. Lee, Appl. Phys. Lett. **85**, 5052 (2004).
[7]W. I. Park, J. S. Kim, G.-C. Yi, and H.-J. Lee, Adv. Mater.(Weinheim, Ger.) **17**, 1393 (2005).
[8]S. Song, W.-K. Hong, S.-S. Kwon, and T. Lee, Appl. Phys. Lett. **92**, 263109 (2008).
[9]P.-C. Chang, Z. Fan, C.-J. Chien, D. Stichtenoth, C. Ronning, and J. G. Lu, Appl. Phys. Lett. **89**, 133113 (2006).
[10]D. Wang, Y.-L. Chang, Q. Wang, J. Cao, D. B. Farmer, R. G. Gordon, and H. Dai, J. Am. Chem. Soc. **126**, 11602 (2004).
[11]S. A. Dayeh, C. Soci, P. K. L. Yu, E. T. Yu, and D. Wang, Appl. Phys. Lett. **90**, 162112 (2007).
[12]Y. Gu, J. P. Romankiewicz, J. K. David, J. L. Lensch, and L. J. Lauhon, Nano Lett. **6**, 948 (2006).
[13]W. I. Park, J. Yoo, D.-W. Kim, G.-C. Yi, and M. Kim, J. Phys. Chem. B **110**, 1516 (2006).
[14]R. Martel, T. Schmidt, H. R. Shea, T. Hertel, and P. Avouris, Appl. Phys. Lett. **73**, 2447 (1998).
[15]S. Sasa, M. Ozaki, K. Koike, M. Yano, and M. Inoue, Appl. Phys. Lett. **89**, 053502 (2006).
[16]X. Jiang, Q. Xiong, S. Nam, F. Qian, Y. Li, and C. M. Lieber, Nano Lett. **7**, 3214 (2007).
[17]Y. Li, J. Xiang, F. Qian, S. Gradečak, Y. Wu, H. Yan, H. Yan, D. A. Blom, and C. M. Lieber, Nano Lett. **6**, 1468 (2006).
[18]S. M. Sze, *Physics of Semiconductor Devices* (Wiley, New York, 1981), Chap. 8.

This article is copyrighted as indicated in the article. Reuse of AIP content is subject to the terms at: http://scitation.aip.org/termsconditions. Downloaded to IP: 141.223.173.110 On: Wed, 22 Apr 2015 05:35:35